Crystallography Reviews

ISSN: 0889-311X (Print) 1476-3508 (Online) Journal homepage: http://www.tandfonline.com/loi/gcry20

Crystal chemistry of organic minerals – salts of organic acids: the synthetic approach

Oscar Enrique Piro & Enrique José Baran

To cite this article: Oscar Enrique Piro & Enrique José Baran (2018) Crystal chemistry of organic minerals – salts of organic acids: the synthetic approach, Crystallography Reviews, 24:3, 149-175, DOI: 10.1080/0889311X.2018.1445239

To link to this article: https://doi.org/10.1080/0889311X.2018.1445239

Published online: 07 Mar 2018.

CRYSTALLOGRAPHY REVIEWS, 2018
VOL. 24, NO. 3, 149–175
https://doi.org/10.1080/0889311X.2018.1445239

Taylor & Francis
Taylor & Francis Group

REVIEW

Crystal chemistry of organic minerals – salts of organic acids: the synthetic approach

Oscar Enrique Piro[a] and Enrique José Baran[b]

[a]Departamento de Física, Facultad de Ciencias Exactas, Universidad Nacional de La Plata and Institute IFLP (CONICET, CCT-La Plata), La Plata, Argentina; [b]Centro de Química Inorgánica CEQUINOR (CONICET-UNLP), Facultad de Ciencias Exactas, Universidad Nacional de La Plata, La Plata, Argentina

ABSTRACT

The term 'organic minerals' means naturally occurring crystalline organic compounds including metal salts of formic, acetic, citric, mellitic, methanesulfonic and oxalic acids. As for the rest of the (inorganic) minerals, the primary tool to disclose their crystal and molecular structure and therefore to understand their mutual relationship with each other and with synthetic analogues and also their physicochemical properties is X-ray diffraction crystallography ever since the dawn of this methodology in 1913. The structure of several synthetic organic minerals was solved well before the discovery of their natural counterpart. On the other hand, complete crystal structure determination of early discovered organic minerals had to await the advent of combined synthetic and advanced X-ray diffraction methods to fully unveil their crystal structures. We review here the crystal chemistry of organic minerals and show the importance of structural studies on their synthetic analogues. This will be highlighted by case studies on the recently reported synthetic novgorodovaite, $Ca_2(C_2O_4)Cl_2{\cdot}2H_2O$, and its heptahydrate analogue, $Ca_2(C_2O_4)Cl_2{\cdot}7H_2O$, and the isotypic to each other stepanovite, $NaMg[Fe(C_2O_4)_3]{\cdot}9H_2O$, and zhemchuzhnikovite, $NaMg[Al_xFe_{1-x}(C_2O_4)_3]{\cdot}9H_2O$.

ARTICLE HISTORY
Received 29 November 2017
Accepted 22 February 2018

KEYWORDS
Organic minerals; synthetic analogues of minerals; natural oxalates; novgorodovaite; stepanovite and zhemchuzhnikovite; advanced X-ray diffraction

1. Introduction

Minerals were the first crystals submitted to structural scrutiny by X-ray diffraction through the pioneering work of W. L. Bragg on alkaline halides, more than one hundred years ago [1]. However, full crystallographic characterization of minerals by diffraction methods is frequently hampered by several drawbacks, including unavailability of natural samples, lack of purity and other disorders of these materials, and the difficulty in finding natural single crystals suitable for detailed structural work.

We show here that synthetic chemistry of mineral analogues followed by single crystal X-ray diffraction employing modern data collection, advanced space group and crystal structure determinations and also routine untwining procedures to disentangle the diffraction intensities in terms of two or more contributing single crystal domains have

CONTACT Oscar Enrique Piro piro@fisica.unlp.edu.ar

the potential to circumvent these shortcomings, providing a wealth of new structural information on the known natural mineral counterparts and on hitherto undiscovered ones.

Advanced space group and crystal structure determination procedures no longer depend on the sometimes unreliable and ambiguous X-ray diffraction extinctions and intensity statistics. Particularly, and based on the empirical fact that (despite the neglect of structural information embodied in the higher symmetry of the correct space group) usually crystal structures yield more easily when solved in the triclinic space group $P1$ [2] and the observation that space groups can be determined from $P1$ structure factor phases [3,4], Sheldrick implemented in SHELXT program [5] an integrated space group and crystal structure determination algorithm, so-called intrinsic phasing. It combines Patterson (and also direct methods) from small-molecule crystallography with density modification and dual-space recycling from macromolecular crystallography and departs from standard structure determination procedures where normally the space group is determined first and the crystal structure afterward. Now, with the only prior knowledge of the Laue group and the atom species expected to be present in the crystal:

(1) The X-ray diffraction data set is expanded to the space group $P1$ where the structure is solved from an initial trial constellation of peaks provided by Patterson superposition methods. This is followed by dual-space recycling to obtain optimal electron density and $P1$ phases.
(2) Let us define $\Delta\mathbf{r}$ as the displacement vector that refers the $P1$ structure to the unit cell origin of the candidate space group G, whose symmetry operations are $(\mathbf{P}_m, \mathbf{t}_m)$, being $\mathbf{P}_m$ the point group operation (a 3×3 matrix) and $\mathbf{t}_m$ the corresponding translation vector, with the suffix m running over the space group members. The 'star' of reciprocal vector $\mathbf{h}$ is defined through the symmetry operation: $\mathbf{h}_m = \mathbf{h}\mathbf{P}_m$. Because the $\Delta\mathbf{r}$ shift, $P1$ phases $\phi(\mathbf{h})$ and $\phi(\mathbf{h}_m)$ change to $\phi'(\mathbf{h}) = \phi(\mathbf{h}) + 2\pi\mathbf{h} \cdot \Delta\mathbf{r}$ and $\phi'(\mathbf{h}_m) = \phi(\mathbf{h}_m) + 2\pi\mathbf{h}_m \cdot \Delta\mathbf{r}$, respectively. Because these phases are symmetry-related in the space group G by $\phi'(\mathbf{h}) - \phi'(\mathbf{h}_m) = 2\pi\mathbf{h} \cdot \mathbf{t}_m$, it turns out that for the correct space group and origin shift,

$$q = \phi(\mathbf{h}_m) - \phi(\mathbf{h}) + 2\pi[\mathbf{h} \cdot \mathbf{t}_m + (\mathbf{h}_m - \mathbf{h}) \cdot \Delta\mathbf{r}], \tag{1}$$

should ideally be zero (module 2π). The departure from this null value is measured by a phase error (α) which varies from 0 to 1 (for random phases).
(3) The phases are first subjected to a centre-symmetric test by scanning for $\Delta\mathbf{r}$ displacements of the $P1$ unit cell origin that bring the shifted phases $\phi'(\mathbf{h}) = \phi(\mathbf{h}) + 2\pi\mathbf{h} \cdot \Delta\mathbf{r}$ the closest to the ideal values of cero or π radians, followed by a measure of the corresponding phase error (α_0). This should be small for a constellation of atoms that possess an inversion centre.
(4) The $P1$ phases are then employed in a full search employing Equation (1) for the correct space group and the translation necessary to refer the electron density to the proper unit cell origin.
(5) The phases are then averaged in every possible space group compatible with the known Laue group and used to calculate improved maps.
(6) The integrated electron density around the peaks of the maps is assigned to the assumed atomic species and thus a chemical formula is proposed.

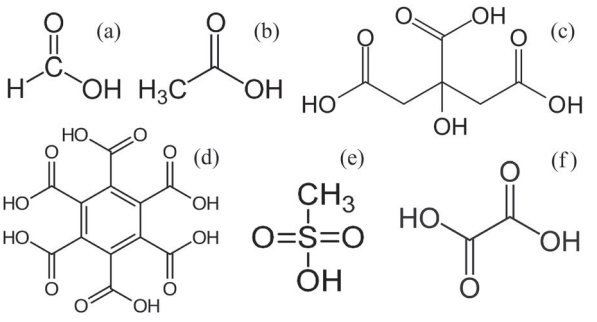

Scheme 1. Mineral forming organic acids: (a) formic; (b) acetic; (c) citric; (d) mellitic; (e) methanesulfonic and (f) oxalic.

(7) The correct space group and structure solution is selected among the trials on the basis of several figures of merit, including the standard agreement $R1$-factor, R_{weak} (average of calculated E^2_{calc} for the 10% of unique reflections with the smallest observed normalized structure factors E_{obs}) and the phase error (α), all of which should be the smallest for the right choose.

The commonly named 'organic minerals' constitute class 10 in the mineralogical classification of Strunz [6] and include simple and complex salts of different organic acids (formic, acetic, citric, mellitic, methanesulfonic and oxalic acids, cf. Scheme 1) as well as numerous crystalline hydrocarbons, some amides, imides, porphyrines, triazolate complexes and other compounds.

The purpose of this review is to present an overview of the crystal chemistry of the natural species derived from the above-mentioned simple organic acids and to emphasize the importance of the investigation on their synthetic analogues for a better understanding of their structural and general physicochemical behaviour.

In Sections 2.1–2.5, we shall review the occurrence and general properties of the selected organic minerals derived from formic, acetic, citric, mellitic and methanesulfonic acids. Section 2.6 will be devoted to the most abundant class of organic minerals, namely the natural oxalates. These structural studies will be highlighted by case studies on synthetic minerals, including the recently reported novgorodovaite, $Ca_2(C_2O_4)Cl_2{\cdot}2H_2O$, and its heptahydrate analogue, $Ca_2(C_2O_4)Cl_2{\cdot}7H_2O$, and the isotypic to each other stepanovite, $NaMg[Fe(C_2O_4)_3]{\cdot}9H_2O$, and zhemchuzhnikovite, $NaMg[Al_xFe_{1-x}(C_2O_4)_3]{\cdot}9H_2O$.

2. Salts of organic acids

The list of the so far known minerals derived from organic acids includes 2 formates, 2 acetates, 1 citrate, 1 mellitate, 1 methanesulfonate and 21 oxalates (cf. Scheme 1). The most important mineralogical, chemical and structural characteristics of these groups are analysed in the following subsections. For convenience, in Tables 1 and 2 we present an overview of crystallographic data of these natural species and their synthetic counterparts.

Table 1. Crystal data for selected organic minerals and their synthetic analogues derived from formic, acetic, citric, mellitic and methanesulfonic acids.

Mineral	Natural	Ref.	Synthetic	Ref.
Formates				
Formicaite $Ca(HCOO)_2$	$P4_12_12_1; Z = 4$ $a = 6.77(1)$ Å $c = 9.50(4)$ Å	[7, 8]	$P4_12_12_1; Z = 4$ $a = 6.765(2)$ Å $c = 9.456(3)$ Å	[9]
Dashkovaite $Mg(HCOO)_2{\cdot}2H_2O$	$P2_1c; Z = 4$ $a = 8.64(1)$ Å $b = 7.15(1)$ Å $c = 9.38(1)$ Å $\beta = 98.0(1)°$	[10–12]	$P2_1c; Z = 4$ $a = 8.640(5)$ Å $b = 7.149(3)$ Å $c = 9.382(7)$ Å $\beta = 98.05(1)°$	[13]
Acetates				
Hoganite $Cu(CH_3COO)_2{\cdot}H_2O$	$C2/c; Z = 8$ $a = 13.162(3)$ Å $b = 8.555(2)$ Å $c = 13.850(3)$ Å $\beta = 117.08(3)°$	[14]	$C2/c; Z = 8$ $a = 13.167(4)$ Å $b = 8.563(8)$ Å $c = 13.862(7)$ Å $\beta = 117.019(2)°$	[15]
Paceite $CaCu(CH_3COO)_4{\cdot}6H_2O$	$I4/m; Z = 4$ $a = 11.155(4)$ Å $c = 16.24(2)$ Å	[14]	$I4/m; Z = 4$ $a = 11.152(2)$ Å $c = 16.240(1)$ Å	[16]
Calclacite $Ca(CH_3COO)Cl{\cdot}5H_2O$			$P2_1/c; Z = 4$ $a = 6.82$ Å $b = 13.72$ Å $c = 11.51$ Å $\beta = 116.42°$	[17]
Citrates				
Earlandite $Ca_3(C_6H_5O_7)_2{\cdot}4H_2O$			$P\bar{1}; Z = 2$ $a = 5.9466(4)$ Å $b = 10.2247(8)$ Å $c = 16.650(1)$ Å $\alpha = 72.213(7)°$ $\beta = 79.718(7)°$ $\gamma = 89.791(6)°$	[18]
Mellitates				
Mellite $Al_2[(C_6(COO)_6]{\cdot}16H_2O$	$I4_1/acd; Z = 8$ $a = 15.53(1)$ Å $b = 23.19(1)$ Å	[19]	$I4_1/acd; Z = 8$ $a = 15.563(1)$ Å b = 23.122(2) Å	[20]
Methanesulfonates				
Ernstburkeite $Mg(CH_3SO_3)_2{\cdot}12H_2O$			$R\bar{3}; Z = 3$ $a = 9.27150(8)$ Å $c = 21.1298(4)$ Å	[21]

2.1. Natural formates

Two formate minerals have been characterized, these are formicaite, $Ca(HCOO)_2$ [7,8] and dashkovaite, $Mg(HCOO)_2{\cdot}2H_2O$ [10–12] and in both cases their characterization was performed by comparisons with the analogous synthetic compounds [7,10].

Formicaite was found in the Solondo boron deposit (Buryatia, Russia) and in the Novofrolovskoye copper deposit (Ural Mountains, Russia). Formicaite and synthetic β-$Ca(HCOO)_2$ have practically identical powder X-ray diffraction patterns as well as identical IR absorption spectra [7,8]. Synthetic calcium formate presents four different crystal modifications, known as α, β, γ and δ forms [9,50,51]. β-$Ca(HCOO)_2$ shows a primitive tetragonal Bravais lattice and its crystal data are detailed in Table 1. The Ca(II) cations are coordinated by six O-atoms, the formate groups are planar and their two C–O distances are significantly different [9].

Table 2. Crystal data for selected organic minerals and their synthetic analogues derived from oxalic acid.

Mineral	Natural	Ref.	Synthetic	Ref.
Natroxalate $Na_2C_2O_4$	$P2_1/a; Z = 2$ $a = 10.426(9)$ Å $b = 5.225(5)$ Å $c = 3.479(3)$ Å $\beta = 93.14(8)°$	[22,23]	$P2_1/c; Z = 2$ $a = 3.449(2)$ Å $b = 5.243(5)$ Å $c = 10.375(4)$ Å $\beta = 92.66(4)°$	[24]
Whewellite $CaC_2O_4{\cdot}H_2O$	$P2_1/c; Z = 8$ $a = 6.290(1)$ Å $b = 14.583(1)$ Å $c = 10.116(1)$ Å $\beta = 109.46(2)°$	[25]	$P2_1/n; Z = 8$ a = 9.9763(3) Å $b = 14.5884(4)$ Å $c = 6.2913(3)$ Å $\beta = 107.08(3)°$	[26]
Weddellite $CaC_2O_4{\cdot}2H_2O$	$I4/m; Z = 8$ $a = 12.371(3)$ Å $c = 7.357(2)$ Å	[25]		
Caoxite $CaC_2O_4{\cdot}3H_2O$	$P\bar{1}; Z = 2$ $a = 6.097(1)$ Å $b = 7.145(1)$ Å $c = 8.434(1)$ Å $\alpha = 76.54(1)°$ $\beta = 70.30(1)°$ $\gamma = 70.75(1)°$	[27]	$P\bar{1}; Z = 2$ $a = 6.1097(13)$ Å b = 7.1642(10) Å $c = 8.4422(17)$ Å $\alpha = 76.43(1)°$ $\beta = 70.19(2)°$ $\gamma = 70.91(2)°$	[28]
Novgorodovaite $Ca_2(C_2O_4)Cl_2{\cdot}2H_2O$	$I2/m; Z = 2$ $a = 6.936(3)$ Å $b = 7.382(3)$ Å $c = 7.443(3)$ Å $\beta = 94.3(1)°$	[29]	$I2/m; Z = 2$ $a = 6.9352(3)$ Å $b = 7.3800(4)$ Å $c = 7.4426(3)$ Å $\beta = 94.303(4)°$	[30]
Glushinskite α-$MgC_2O_4{\cdot}2H_2O$			$C2/c; Z = 4$ $a = 12.68$ Å $b = 5.39$ Å $c = 9.97$ Å $\beta = 129.5°$	[31]
Oxammite $(NH_4)_2C_2O_4{\cdot}H_2O$			$P2_12_12; Z = 2$ $a = 8.035(4)$ $b = 10.309(4)$ $c = 3.795(2)$	[32]
Lindbergite α-$MnC_2O_4{\cdot}2H_2O$	$C2/c; Z = 4$ $a = 11.995(5)$ Å $b = 5.632(2)$ Å $c = 9.967(7)$ Å $\beta = 128.34(4)°$	[33]	$C2/c; Z = 4$ $a = 11.765(1)$ Å $b = 5.6550(6)$ Å $c = 9.637(1)$ Å $\beta = 125.843(6)°$	[34]
Falottaite $MnC_2O_4{\cdot}3H_2O$	$Pcaa; Z = 4$ $a = 10.527(5)$ Å $b = 6.626(2)$ Å $c = 9.783(6)$ Å	[33]	$Pcca; Z = 4$ $a = 9.7660(9)$ Å $b = 6.6155(6)$ Å $c = 10.519(1)$ Å	[35]
Moolooite $CuC_2O_4{\cdot}nH_2O$			$P2_1/n; Z = 2$ $a = 5.9598(1)$ Å $b = 5.6089(1)$ Å $c = 5.1138(1)$ Å $\beta = 115.320(1)°$	[36]
Wheatleyite $Na_2Cu(C_2O_4)_2{\cdot}2H_2O$	$P\bar{1}; Z = 1$ $a = 7.559(3)$ Å $b = 9.665(4)$ Å $c = 3.589(1)$ Å $\alpha = 76.65(2)°$ $\beta = 103.67(2)°$ $\gamma = 109.10(2)°$	[37]	$P\bar{1}; Z = 1$ $a = 7.536(3)$ Å $b = 9.473(4)$ Å $c = 3.576(2)$ Å $\alpha = 81.90(6)°$ $\beta = 103.77(5)°$ $\gamma = 108.09(4)°$	[38]

(*continued*).

Table 2. Continued.

Mineral	Natural	Ref.	Synthetic	Ref.
Antipinite $NaK_3Cu_2(C_2O_4)_4$	$P\bar{1}; Z = 2$ $a = 7.1574(5)$ Å $b = 10.7099(8)$ Å $c = 11.1320(8)$ Å $\alpha = 113.093(1)°$ $\beta = 101.294(1)°$ $\gamma = 90.335(1)°$	[39]		
Humboldtine $Fe(C_2O_4)\cdot 2H_2O$			C2/c; $Z = 4$ $a = 12.01(1)$ Å $b = 5.557(5)$ Å $c = 9.920(9)$ Å $\beta = 128.53(3)°$	[40]
Minguzzitte $K_3[Fe(C_2O_4)_3]\cdot 3H_2O$			$P2_1/c; Z = 4$ $a = 7.742(1)$ Å $b = 19.917(1)$ Å $c = 10.346(1)$ Å $\beta = 107.85(1)°$	[41]
Stepanovite $NaMg[Fe(C_2O_4)_3]\cdot 9H_2O$	Unknown; $Z = 6$ $a = 9.85$ Å $c = 36.67$ Å	[42,43]	P3c1; $Z = 6$ $a = 17.0483(4)$ Å $c = 12.4218(4)$ Å	[44]
Zhemchuzhnikovite $NaMg[Al_xFe_{1-x}(C_2O_4)_3]\cdot 9H_2O$	Unknown; $Z = 6$ $a = 16.67(5)$ Å $c = 12.51(3)$ Å	[42,43]	P3c1; $Z = 6$ $a = 16.8852(5)$ Å $c = 12.5368(5)$ Å	[44]
Coskrenite $(Ce,Nd,La)_2(SO_4)_2(C_2O_4)\cdot 8H_2O$	$P\bar{1}; Z = 1$ $a = 6.007(1)$ Å $b = 8.361(2)$ Å $c = 9.189(2)$ Å $\alpha = 99.90(2)°$ $\beta = 105.55(2)°$ $\gamma = 107.71(2)°$	[45]		
Levinsonite-(Y) $(Y,Nd,Ce)Al(SO_4)_2(C_2O_4)\cdot 12H_2O$	P2/n; $Z = 2$ $a = 10.289(1)$ Å $b = 9.234(1)$ Å $c = 11.015(1)$ Å $\beta = 108.50(1)°$	[46]		
Zugshunstite-(Ce) $(Ce,Nd,La)Al(SO_4)_2(C_2O_4)\cdot 12H_2O$	C2/c; $Z = 4$ $a = 8.718(1)$ Å $b = 18.313(2)$ Å $c = 13.128(2)$ Å $\beta = 93.90(1)°$	[46]		
Deveroite-(Ce) $Ce_2(C_2O_4)_3\cdot 10H_2O$	$P2_1/c; Z = 2$ $a = 11.240(8)$ Å $b = 9.64(1)$ Å $c = 10.34(1)$ Å $\beta = 114.4(1)°$	[47]	$P2_1/c; Z = 2$ $a = 11.347$ Å $b = 9.630$ Å $c = 10.392$ Å $\beta = 114.52°$	[48]
Kyanoxalite $Na_{6.4}K_{0.6}[Al_6Si_6O_{24}](C_2O_4)_{0.5}(H_2O)_{4.4}$	$P6_3; Z = 1$ $a = 12.6792(6)$ Å $c = 5.1772(2)$ Å	[49]		

The second formate mineral, dashkovaite, was found in the Korshunovskoye boron deposit in the Irkutsk district (Siberia, Russia). It is practically identical to synthetic $Mg(HCOO)_2\cdot 2H_2O$ in composition, powder X-ray diffraction pattern and physical properties [10–12]. The structure of the synthetic material was determined at 130 and 293 K. It crystallizes in the monoclinic system (cf. Table 1) with two structurally different Mg(II) ions in the lattice; one of them is coordinated by six O-atom from formate anions, whereas

the second one is surrounded by four O-atoms from water molecules and two O-atoms from formate groups. The coordination polyhedra are, in both cases, close to a perfect octahedron [13].

2.2. Natural acetates

The two known natural acetates, namely hoganite, $Cu(CH_3COO)_2{\cdot}H_2O$, and paceite, $CaCu(CH_3COO)_4{\cdot}6H_2O$, were found some years ago in the Potosi Mine, Broken Hill (New South Wales, Australia), associated with goethite, hematite, quartz, azurite and cerusite, along with some other phases [14]. Both acetates constitute typical examples of binuclear M(II) complexes (Cu(II) in the case of hoganite or Cu(II)/Ca(II) in the case of paceite), with four carboxylate bridges [52].

The structure of hoganite was determined by single crystal X-ray diffraction in the centred monoclinic lattice [14] and the structure of the related synthetic complex was first resolved in 1953 [53] and later refined by neutron diffraction [15]. The structural data of this complex are clearly in agreement with those reported for hoganite.

Also in the case of paceite, the crystallographic data, obtained in this case by powder X-ray diffraction [14], are in satisfactory agreement with data reported for the synthetic material [16] as shown in Table 1.

Another species related to the two mentioned acetates is calclacite, $Ca(CH_3COO)Cl{\cdot}5H_2O$, although it is not a natural species but essentially a museum artefact [14]. It is found in the form of efflorescences on certain calcareous rocks stored in wooden cases. As the same rocks when stored in glass showed no formation of efflorescences, it was concluded that the acetic acid was probably derived from the wood and, therefore, calclacite cannot be classed as a mineral in the strict sense [54]. Structural data for a synthetic sample were initially reported by van Tassel [55] and a most complete structural analysis performed later by Giuseppetti et al. [17]. Calclacite crystallizes in the monoclinic system (cf. Table 1) and presents much distorted CaO_8 units, linked through edges that generate infinite chains nearly parallel to the crystal [100] direction [17].

2.3. Natural citrates

Only one natural citrate is so far known. It is the rare mineral earlandite, which was identified in the form of polycrystalline nodules in the ocean bottom of the Weddel Sea (Antarctica) and characterized as the tetrahydrate of calcium citrate [56]. It constitutes an example of new structural information provided by combined synthetic and advanced X-ray diffraction methods to remove the uncertainties associated with natural samples and technical limitations of old instruments. In fact, Pogainis et al. [57] determined the mineral to probably belong to the orthorhombic system with unit cell dimensions $a = 30.84$ Å, $b = 10.56$ Å, and $c = 5.92$ Å. The Handbook of Mineralogy lists tricalcium citrate tetrahydrate to be monoclinic with $a = 30.94$ Å, $b = 5.93$ Å, $c = 10.56$ Å and $\beta = 93.74°$ [42]. Complete structural information on this interesting mineral, $[Ca_3(C_6H_5O_7)_2(H_2O)_2]{\cdot}2H_2O$, was only obtained very recently from the study of a synthetic sample [18]. The structure was solved employing X-ray diffraction data (collected with an area detector on a four-circle diffractometer) from pseudo-merohedrically twinned crystals of the synthetic analogue of earlandite. The correct crystal system turned out to be triclinic (see crystal data details in

Table 1). The observed three-dimensional network is dominated by eight-fold-coordinated Ca^{2+} cations linked by citrate anions and hydrogen bonds between two non-coordinating crystal water molecules and two coordinating water molecules.

2.4. Natural mellitates

Mellite, the aluminium (III) salt of mellitic acid (cf. Scheme 1) is so far the only known natural mellitate. It is a very unusual compound in being the sole natural crystalline mineral salt to contain a benzene ring. It is found associated with brown coal and lignite, in different regions of middle Europe and Russia [58]. The crystals are semi-transparent with a honey-yellow colour, from which the mineral takes its German name *Honigstein*. First structural studies were performed by Barth and Ksanda, which correctly concluded that the mineral belongs to the tetragonal crystal system but failed in the assignment of the correct number of water molecules [58].

The structure of mellite, finally determined on a sample collected in Arten (Thuringia, Germany), shows that the correct chemical composition is $Al_2[(C_6(COO)_6]\cdot 16H_2O$ and crystallizes in the body-centred tetragonal Bravais lattice [19]. It was demonstrated recently that the single crystal structure and IR spectra of natural mellite and of its synthetic counterpart were identical [20]. A detailed analysis of the Raman dispersion spectra of mineral samples has also been recently published [59].

2.5. Natural methanesulfonates

So far only one salt of methanesulfonic acid was found as a mineral, namely ernstburkeite, $Mg(CH_3SO_3)_2\cdot 12H_2O$. It occurs as solid inclusions, typically with a grain size up to 5 μm, hosted in ice in an Antarctic glacial core with gypsum and ice as associated minerals [60]. Methanesulfonic acid is probably formed by the oxidation of dimethylsulfoxide (generated by processes involving phytoplankton) in the atmosphere. Later, it is deposited in ice cores as methanesulfonate salts, probably due to its fixation on alkaline particles of marine or continental origin during the glacial period [60].

This is another paradigmatic example showing the value of the synthetic approach to the crystal chemistry of minerals dealt with in this review. In fact, the mineral grows as micro-sized and impure crystals embedded in ice, too small for detailed structural X-ray diffraction studies with in-lab radiation sources. In contrast, it was feasibly to grow pure and well-faceted synthetic single crystals, measuring tenths of a millimetre in size, which afforded the full molecular structure to be determined from low-temperature data collected on a Nonius Kappa CCD diffractometer with a rotating anode X-ray source [21]. Among other techniques, the identity of ernstburkeite with its synthetic analogue was assessed by Raman spectroscopy. The analogue crystallizes in the trigonal space group $R\bar{3}$ with $Z = 3$ (cf. Table 1). The metal ion is on a crystallographic $\bar{3}(S_6)$ site symmetry in an octahedral environment, coordinated to six, symmetry-related, water molecules, conforming an hydrated $[Mg(H_2O)_6]^{2+}$ cation. The methanesulfonate $CH_3SO_3^-$ anion is on a three-fold (C_3) rotation axis. The shell of water molecules surrounding the metal ion prevents its direct contact with the $CH_3SO_3^-$ ion, which instead acts as acceptor of an OwH ... O bond with the coordinated-to-metal water molecule. This gives rise to a layered structure perpendicular to the trigonal axis. Neighbouring layers, in turn, are bridged to each other

through H-bonding involving the remaining, crystallization, water molecule. The structural results show that the salt is better described by the $[Mg(H_2O)_6](CH_3SO_3)_2.6H_2O$ chemical formula [21].

2.6. Natural oxalates

As mentioned in the opening paragraph of this Section, there are 21 natural oxalate minerals so far found and described. Therefore, oxalates constitute the most abundant class of organic minerals, being also widely distributed in Nature and having been observed in rocks, soil, water bodies and among a variety of living organisms, including plants and animals (the so-called *biominerals*) [31,61,62].

2.6.1. Alkaline, alkaline-earth and ammonium oxalates

The only known natural alkaline oxalate is natroxalate, $Na_2C_2O_4$, found as a hydrothermal phase in hyperagpaitic pegmatites of the Lovozero alkaline massif, Kola Peninsula, Russia, where it is associated with aegirine, albite, elpidite and other minerals. It occurs as granular nodules, as vein let-like segregations, as columnar crystals and as radiating aggregates and presents monoclinic symmetry, by analogy to the synthetic material, as determined from the powder pattern and detailed in Table 2 [22,23].

The crystal structure of synthetic lithium oxalate was solved by Beagley and Small [63] from combined Weissenberg photographic and semi-automatic three-circle diffractometer data, employing Patterson and Fourier methods. It crystallizes in the monoclinic space group $P2_1/n$ with $a = 3.400(1)$ Å, $b = 5.156(2)$ Å, $c = 9.055(3)$ Å, $\beta = 95.36(1)°$ and $Z = 2$. The oxalate anion is on a crystallographic inversion centre; it is planar to within experimental accuracy and shows an anomalously long C–C bond length (1.564(2) Å). The small ionic radius of lithium limits the number of ligand atoms in the metal coordination sphere before strong steric ligand–ligand repulsion effect (crowding) sets in. In fact, in $Li_2C_2O_4$ the lithium ion is in a distorted tetrahedral environment (LiO_4 core).

The structural characterization of synthetic $Na_2C_2O_4$ is previous to the discovery of the mineral species (natroxalate). The structure was first reported by Jeffrey and Parry [64], employing X-ray diffraction intensities visually estimated from Weissenberg photographs and the structure solved in projections onto the (010) and (001) crystal planes by Patterson and Fourier synthesis from (*h*0*l*) and (*hk*0) intensities, and later refined by Reed and Olmstead [24] from data collected at 140 K with a Syntex $P2_1$ diffractometer (cf. Table 2). The oxalate ion is planar to within experimental accuracy and shows an anomalously long C–C bond length (1.568(4) Å) hinting to an σ-bond of formal order slightly less than one and therefore to some degree of rotational freedom around the bond. This, in turn, suggests that, contrary to observation, the staggered, not the planar, conformation should be preferred. Because crowding effects of oxalalate oxygen ligand around the small-sized sodium ion, the metal is in a distorted octahedral, NaO_6, coordination. Dinnebier et al. [65] undertook the synthesis and structural study of the other, heavier, members of the anhydrous alkali metal oxalates, namely isotypic $K_2C_2O_4$ and $Rb_2C_2O_4$-β (orthorhombic *Pbam*) and isotypic $Rb_2C_2O_4$-α and $Cs_2C_2O_4$ (monoclinic $P2_1/c$). Because the growing of single crystals adequate for X-ray diffraction proved elusive, the authors resorted to structural powder X-ray diffraction to rationalize the above-mentioned fact observed in $Na_2C_2O_4$ and also in the majority of hydrated alkali and alkali-earth oxalate salts, namely that oxalate presents

a strictly or near planar conformation in the crystal lattice when the staggered one should be preferred on account of its intra-molecular bonding structure. They concluded that the conformation of the oxalate anion, when acting as a weak interacting ligand, is mainly determined by packing effects: bonded to relative large-radius, non-polarizing cations K^+, Rb^+ and Cs^+, the planar as well as the much rarer staggered conformations have been observed.

The alkali oxalates show a strong correlation between alkali ionic radii [$r(Li^+) < r(Na^+) < r(K^+) < r(Rb^+) < r(Cs^+)$] and coordination number around the metal. In fact, environmental oxygen atoms being equal to 4 for the smallest lithium ion (tetrahedral LiO_4 core), increasing to 6 for sodium (octahedral NaO_6 core), 8 for isotypic potassium and β-rubidium phase (cubic KO_8 and RbO_8 cores) and 9 and 10 for isotypic caesium and α-rubidium phase.

Calcium oxalate minerals (the mono-, di- and tri-hydrates of CaC_2O_4, known as whewellite, weddellite and caoxite, respectively) are the most common family of organic minerals present in natural environments, usually occurring in carbonate concretions, marine and lake sediments, hydrothermal veins and lignite [61]. They are also the most common and abundant class of biominerals found in the plant kingdom [31,61,62,66–69].

By far, the most common calcium oxalate mineral in all environments is whewellite, while weddellite is subordinate and the even rarer caoxite is only found sporadically. This fact can probably be related to the extremely low water solubility of whewellite (its solubility product is only 1.45×10^{-9} [70]). On the other hand, it is also the thermodynamically most stable form of the hydrates of calcium oxalate [31,61,62]. Interestingly, it is dimorphic, presenting a basic structure, which is stable above 38°C (monoclinic, space group $C2/m$ and $Z = 4$) and a low temperature (derivative) form, which is a superstructure generated by doubling of the b unit cell constant of the basic form (monoclinic, space group $P2_1/c$ and $Z = 8$) [25,26,31, 71].

In weddellite, usually formulated as $Ca(C_2O_4)\cdot(2+x)H_2O$, the fractional waters of hydration (i.e. x in the chemical formula) are of zeolitic nature and do not contribute to the Ca(II) coordination polyhedral [25,31]. A most recent study suggested that the end-member formula for weddellite should be given as $Ca(C_2O_4)\cdot(2.5 - x)H_2O$, where $0 \leq x \leq 0.25$ [72].

Calcium oxalate trihydrate, the synthetic analogue of caoxite, was known [73] well before the discovery of the mineral in 1997. Mainly because it is believed to be a precursor in the formation of kidney stones, its physicochemical characterization is of great interest in the field of human pathology. The first structural analysis by X-ray diffraction was reported by Deganello et al. [74], the molecular model better refined latter from the newly discovered natural samples by Basso et al. [27] and the vibration behaviour (by Raman and FTIR spectroscopy) of the synthetic analogue recently described in Conti *el al.* [28], where it is compared with the spectroscopic signature of the other two hydrates for quick identification purposes. The fast identifying capability of vibration spectroscopy (IR and Raman) is well recognized and some mineral databases include spectral data along with crystallographic information [75].

From the structural point of view, the three calcium oxalates show some strong similarities, as in all of them the Ca(II) ions are coordinated by eight oxygen atoms, belonging either to oxalate anions or to H_2O molecules, located at the corners of a distorted square antiprism [31]. A comparison of these structures show that progression from monohydrate

to dihydrate and trihydrate is a one-to-one-expression of the number of O-atoms contributed by H_2O molecules to the 8-oxygen polyhedron around Ca(II). The transformation of each hydrate to the next lower one implies simply the successive replacement of a water molecule by an oxalate anion (contributing one O-atom) [25,31,74]. The water molecules play, obviously, an important role in the formation of hydrogen bonds which have a strong impact on the overall structural characteristics of all these hydrates.

Apart from the mentioned hydrated calcium oxalates, a fourth, rarer calcium oxalate, was found in 2001 in the Chelkar salt dome, western Kazakhstan, associated with anhydrite, gypsum, halite, bishofite, magnesite and hilgardite. Its crystallographic structural analysis was consistent with the idealized formula $Ca_2(C_2O_4)Cl_2{\cdot}2H_2O$ and the name novgorodovaite was approved for this new mineral [29].

Interestingly, the synthesis of an analogue of novgorodovaite as well as a higher hydrate that arises in the same preparation, namely $Ca_2(C_2O_4)Cl_2{\cdot}7H_2O$, the characterization of their crystal morphologies by optical means and information on crystal *d*-spacing by powder X-ray diffraction, were first reported in 1946 by Jones and White [76]. Recently, we have investigated by single crystal X-ray diffraction the structure of the synthetic analogue of the mineral and also the related heptahydrate and obtained a very clear picture of their structural relationship and individual peculiarities [30].

We found that synthetic $Ca_2(C_2O_4)Cl_2{\cdot}2H_2O$ is identical to novgorodovaite, an identity further confirmed by the comparison between their respective IR absorption and Raman dispersion spectra. It crystallizes in a centred monoclinic lattice (see Table 2) and an ORTEP [77] drawing of the crystal packing is shown in Figure 1.

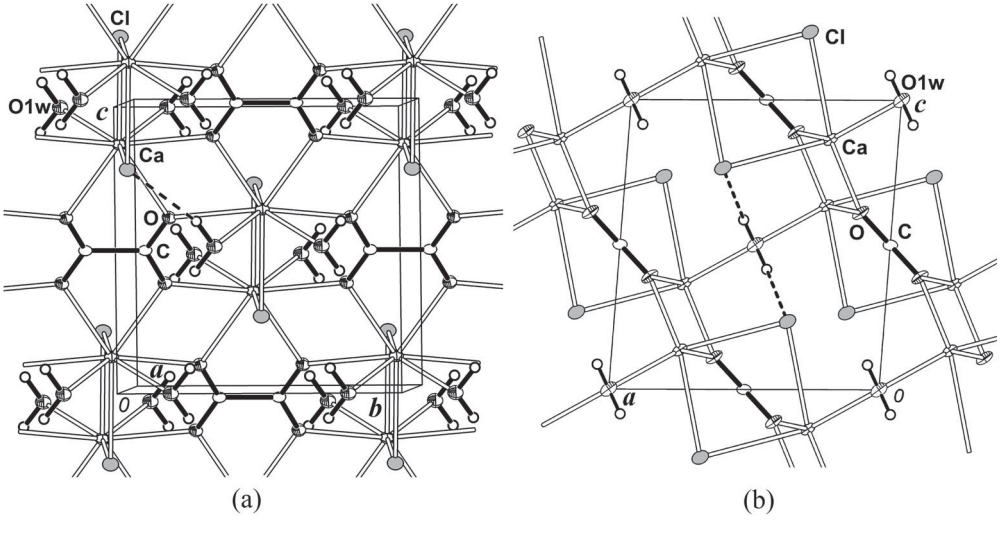

Figure 1. Crystal packing projections of synthetic analogue of novgorodovaite, $Ca_2(C_2O_4)Cl_2{\cdot}2H_2O$, showing the labelling of the non-H atoms and their displacement ellipsoids at the 50% probability label: (a) down the *a*-axis; (b) down the *b*-axis. Carbon, oxygen, calcium and chloride atoms are, respectively, shown by open, hatched, crossed and greyed ellipsoids. For clarity, only a few OwH . . . Cl bonds are shown (by dashed lines). Drawing reproduced from Figure 1 of [30] with permission kindly granted by Springer.

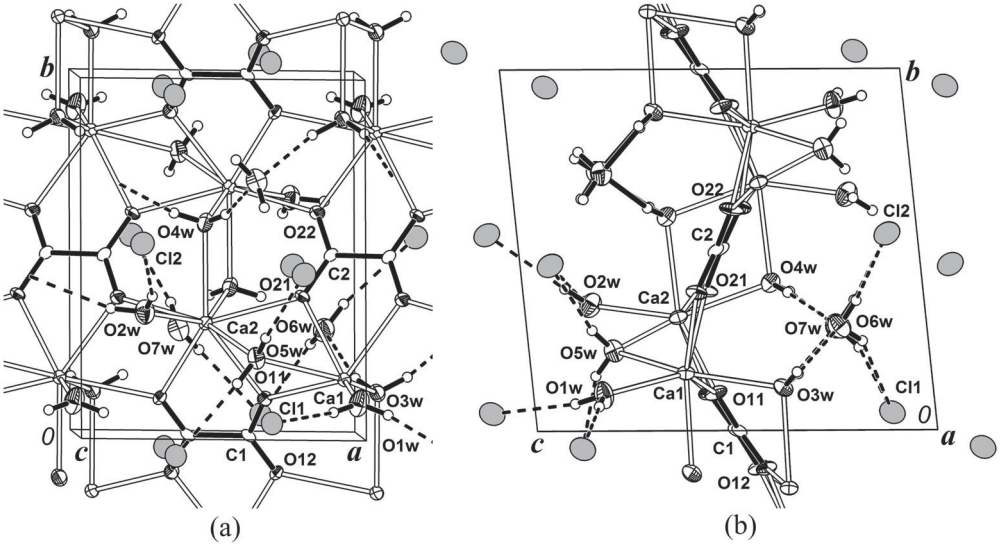

Figure 2. Crystal packing projections of $Ca_2(C_2O_4)Cl_2{\cdot}7H_2O$: (a) down the *c*-axis; (b) down the *a*-axis. Drawing reproduced from Figure 2 of [30] with permission of Springer.

All but the oxalate oxygen and water hydrogen atoms are at special crystal positions. The oxalate anion is at a site of C_{2h} point group symmetry and therefore the $(C_2O_4)^{2-}$ ion is strictly planar. The calcium ion is in a distorted eight-fold polyhedral coordination with four carboxylic oxygen (O) atoms of neighbouring oxalate ions, two water oxygen (Ow) molecules and two chlorine (Cl) ions ($CaO_4Ow_2Cl_2$ core). The crystallographic results show that the chemical formula $Ca_2(C_2O_4)Cl_2{\cdot}2H_2O$ proposed for novgorodovaite [29] is more appropriated than the $Ca(C_2O_4).CaCl_2{\cdot}2H_2O$ formula reported in the early work [76] when the crystal structure was not known. The $Ca_2(C_2O_4)Cl_2{\cdot}2H_2O$ crystal is further stabilized by a OwH ... Cl bond rather that the weak OwH ... O(ox) reported in [29].

The heptahydrate analogue, $Ca_2(C_2O_4)Cl_2{\cdot}7H_2O$, crystallizes as a triclinic twin in the space group $P\bar{1}$ with $a = 7.3928(8)$ Å, $b = 8.9925(4)$ Å, $c = 10.484(2)$ Å, $\alpha = 84.070(7)°$, $\beta = 70.95(1)°$, $\gamma = 88.545(7)°$ and $Z = 2$. A view of the crystal packing is displayed in Figure 2.

There are two independent calcium and oxalate ions, these latter molecules being on crystallographic inversion centres. Though not forced by crystal symmetry as in novgorodovaite, the $(C_2O_4)^{2-}$ anions are planar to within experimental accuracy.

As for the mineral, both calcium ions in the higher hydrate are in an eight-fold environment, but now a pair of water molecules replaces the chlorine ions on the alkaline-metal coordination sphere. In fact, the metals are coordinated to four oxalate oxygen and four water oxygen atoms (CaO_4Ow_4 polyhedron).

The crystal packing of both calcium oxalate-chloride double salts favours the directional bonding of oxalate $(C_2O_4)^{2-}$ ligands to calcium ions through the oxygen sp^2 electron lone pairs as do other related calcium oxalate minerals. In fact, the planar oxalate ions behave in the crystals as molecular spacers both perpendicularly to the –OOC-COO– axis, acting as bidentate ligands, and also along this axis. This latter bonding gives rise to a polymeric

structure which is common to both hydrates and explains the nearly equal cell constants which happen to be coincident with the chain repeatability (monoclinic $b \approx$ triclinic a). When compared with novgorodovaite, the higher water content of $Ca_2(C_2O_4)Cl_2{\cdot}7H_2O$ makes for the major differences observed in their structures and physical properties. In fact, while keeping the above-mentioned Ca ... $(C_2O_4)^{2-}$ directional bonding, the highly polar water molecules displace the chlorine ions from the eight-fold calcium coordination sphere and also surround them through OwH...Cl bonds to prevent the Ca^{2+} ... Cl^- close electrostatic contact observed in novgorodovaite. As a result of the above interactions, the $Ca_2(C_2O_4)Cl_2{\cdot}7H_2O$ solid is arranged in $Ca_2(C_2O_4)(H_2O)_5$ slabs parallel to (001) crystal plane, interspaced by hydrated chlorine slabs (see Figure 2(b)), a layered structure that accounts for (001) to be both an easily cleavage and a twinning plane.

Apart from the discussed calcium oxalates, the dihydrated magnesium oxalate, $MgC_2O_4{\cdot}2H_2O$, known as glushinskite, also plays a relatively important role in nature as it has been found repeatedly as a biomineral in the plant kingdom [62]. This biomineral belongs to one of the most interesting series of metallic oxalate complexes, i. e. the well-known $M^{II}C_2O_4{\cdot}2H_2O$ series with M^{II} = Mg, Fe, Co and Ni, which present two polymorphic forms called α-modification (monoclinic, space group $C2/c$, $Z = 4$) and β-modification (orthorhombic, space group $Cccm$, $Z = 8$). In the case of M^{II} = Mn and Zn only the α-modification has been identified, although for manganese other different complex species (γ-$MnC_2O_4{\cdot}2H_2O$ and $MnC_2O_4{\cdot}3H_2O$) are known [31,62].

A natural ammonium oxalate, known as oxammite, has been found in some guano deposits, associated with certain other (sulphate) minerals [78]. The synthesis of this oxalate, generated as the monohydrate, $(NH_4)_2C_2O_4{\cdot}H_2O$, is very easy and its structure (orthorhombic, space group $P2_12_12$, $Z = 2$) has been reported by different authors [31]. These studies were later complemented by combined neutron and X-ray diffraction study on protonated and fully and partially deuterated crystal forms, aiming to disclose the bonding and lone-pair electron distribution, through N-X maps, along with isotope effects [32]. Besides inter-ionic interactions, the crystal is further stabilized by an extended H-bond network where the oxalate anion acts as acceptor of eight H-bonds, nearly along its oxygen electron lone-pair lobes, from neighbouring ammonium and water molecules donors. These molecules in turn are both in tetrahedral H-bonding environments. The H-bonding observed in $(NH_4)_2C_2O_4{\cdot}H_2O$ is considered to be the cause of oxalate carboxyl planes to be twisted (in about 29°) from each other.

2.6.2. Manganese and copper oxalates

Only two natural Mn(II) oxalates are so far known. These are lindbergite, α-$MnC_2O_4{\cdot}2H_2O$ and falottaite, $MnC_2O_4{\cdot}3H_2O$. The first one was found and investigated from a deposit in Minas Gerais (Brazil) associated with some phosphate minerals. Previous reports also suggested its occurrence in some regions of the Black Forest (Germany), Switzerland and Virginia (USA) [33]. Crystallographic data, obtained by powder X-ray diffraction, are in close agreement with that of synthetic samples of the mineral, as shown in Table 2 [34,79].

On the other hand, the presence of falottaite was detected in the Falotta mine, Oberhalbstein, Grisons (Switzerland) during the summer of 1977 [33,80,81]. It occurs on small quartz crystals, associated with braunite and other manganese minerals. This trihydrate is relatively unstable turning into the dihydrate [33], as also found to be the

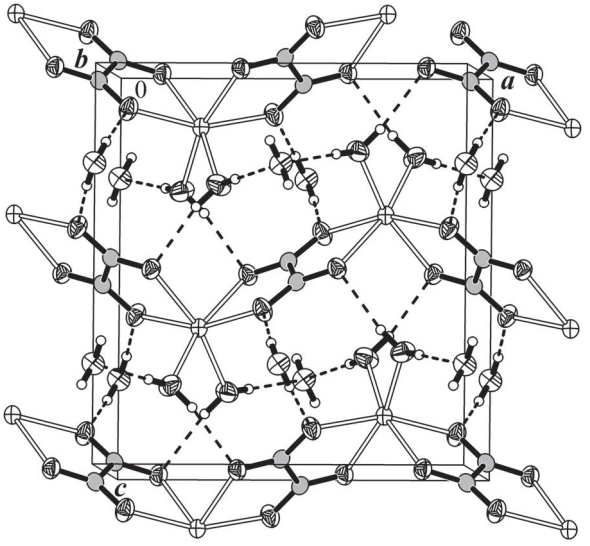

Figure 3. Crystal packing projection down the *b*-axis of synthetic analogue of falottaite, $[Mn(C_2O_4)(H_2O)_2]\cdot H_2O$, showing the non-H atom displacement ellipsoids at the 50% probability label. Carbon, oxygen and manganese atoms are, respectively, shown by open grey, hatched and crossed ellipsoids. H-bonds are indicated by dashed lines. Atomic parameters were taken from [35].

case for the analogous synthetic sample [79]. Its powder X-ray diffractogram coincides with that of the synthetic material [33,79]. Only very recently detailed structural analyses for this oxalate was performed on synthetic samples [35], and show that it should be rather formulated as $[Mn(C_2O_4)(H_2O)_2]\cdot H_2O$, with two water molecules coordinated to manganese(II) and the third one being a crystallization water, as shown in Figure 3. It crystallizes in the orthorhombic space group *Pcca* with $Z = 4$. The Mn(II) ions is sited on a crystallographic two-fold axis in a octahedral environment (MnO_6 core), coordinated to two symmetry-related, oxalate molecules acting as bidentate ligands through the oxygen atoms of their opposite carboxylic groups in a two-bladed propeller-like conformation and along one electron pair lobe on each oxygen ligand. The other two coordination sites are occupied by water oxygen atoms. The well-known bridging capability of the oxalate dianion is here fully exploited by its bridging of neighbouring metal ions to conform a one-dimensional $\{[Mn(C_2O_4)(H_2O)_2]\cdot H_2O\}_n$ chain. Neighbouring chains are linked through OwH ... O(ox) bonds giving rise to a layered structure. The MnO_6 bond geometry and metrics around the metal are consistent with the oxalate and water molecules being weak field ligands giving rise to the paramagnetic high-spin ($S = 5/2$) electronic ground state exhibited by the $Mn(C_2O_4)(H_2O)_2$ complex, as probed by magnetic susceptibility. The one-dimensional $\{[Mn(C_2O_4)(H_2O)_2]\cdot H_2O\}_n$ arrangement of coupled paramagnets explains its observed long-range anti-ferromagnetic behaviour [82].

In the case of copper, three oxalate minerals have so far been described, namely moolooite, $CuC_2O_4\cdot nH_2O$, wheatleyite, $Na_2Cu(C_2O_4)_2\cdot 2H_2O$, and antipinite, $KNa_3Cu_2(C_2O_4)_4$.

Moolooite, probably generated by interaction of oxalic acid from bird guano and copper sulphides, was found in a Western Australia deposit associated with gypsum, silica,

atacamite, whewellite, libethenite and other minerals [83]. The powder X-ray diffraction pattern and the IR spectrum are similar to the corresponding ones of a synthetic copper oxalate hydrate prepared by reaction of solutions of copper acetate and oxalic acid. The water is of zeolitic nature [83]. Preliminary structural information was only obtained by means of EXAFS studies involving the copper environment, as it was difficult to prepare single crystals adequate for X-ray diffraction studies [61,84]. Hampered by this difficulty and, additionally, by conflictive data concerning the water content, Christensen et al. [36] undertook 'a tour de force' to propose a crystal structure for anhydrous CuC_2O_4. To this purpose, the authors employed powder neutron and conventional and synchrotron X-ray diffraction, taking into account crystal micro size and strain effects, and also thermo-gravimetric and thermal decomposition analysis and magnetic susceptibility vs. temperature data. They concluded that synthetic moolooite crystallizes in the space group $P2_1/n$ with $Z = 2$ (cf. Table 2) and advanced a molecular model, based on local structural EXAFS data on Cu–O and Cu ... Cu distances, where Cu(II) ions are at the centre of an elongated octahedral environment, equatorially coordinated at short Cu–O bond distances to the carboxyate oxygen atoms of oxalate molecules acting as spacers in a ... $Cu(C_2O_4)Cu(C_2O_4)$ ... , ribbon-like, chain structure. The six-fold coordination around copper is completed at the apical positions by an oxalate oxygen atom of neighbouring chains that run parallel above and below the ribbon.

The rare mineral wheatleyite, an hydrated sodium copper oxalate, probably generated by oxalic acid of animal origin and mine ground waters, was found in an abandoned mine located near Phoenixville (Chester County, Penn., USA), associated to galena, sphalerite, quartz and a powdered lead oxalate [37]. As shown in Table 2, the unit cell parameters determined for the mineral sample are in good agreement with those obtained for the synthetic complex [38]. It is interesting to comment that analogous complexes, containing K^+, Rb^+, Cs^+ or NH_4^- instead of Na^+, can also be easily prepared and show structures closely related to that of wheatleyite [31].

The most recently characterized copper oxalate is antipinite, $NaK_3Cu_2(C_2O_4)_4$, found in a guano deposit located on the Pabellón de Pica Mountain (Iquique, Tarapacá, Chile), associated with halite, salammoniac, chanabayaite, joanneumite and clays. It is surely generated by the interaction of oxalate, originated in guano, and oxidized chalcopyrite [39]. Its crystal structure was determined by single crystal X-ray diffraction, showing that the mineral belongs to the triclinic space group $P\bar{1}$ with the cell constants reported in Table 2 [39].

2.6.3. Iron oxalates

Four natural iron oxalates are so far known. These are humboldtine, α-$Fe^{II}(C_2O_4)\cdot 2H_2O$, minguzzite, $K_3[Fe^{III}(C_2O_4)_3]\cdot 3H_2O$, stepanovite, $NaMg[Fe^{III}(C_2O_4)_3]\cdot 8\text{-}9H_2O$, and zhemchuzhnikovite, $NaMg[(Al,Fe^{III})(C_2O_4)_3]\cdot 8H_2O$. Only the first one is a ferrous compound whereas the other three, more complex systems, contain ferric iron [31,85].

Humboldtine is one of the oldest known oxalate minerals, initially found in Kolowserux, Bohemia, later at different regions of Germany, the Czech Republic, England and Canada and also in some locations of the Elba Island (Italy), associated with brown coal or iron oxides, and most recently in pegmatite fractures, associated with hematite, magnetite and goethite in Minas Gerais (Brazil) [85]. Structural studies of the mineral were reported by different authors and a definitive structural analysis was performed by single crystal

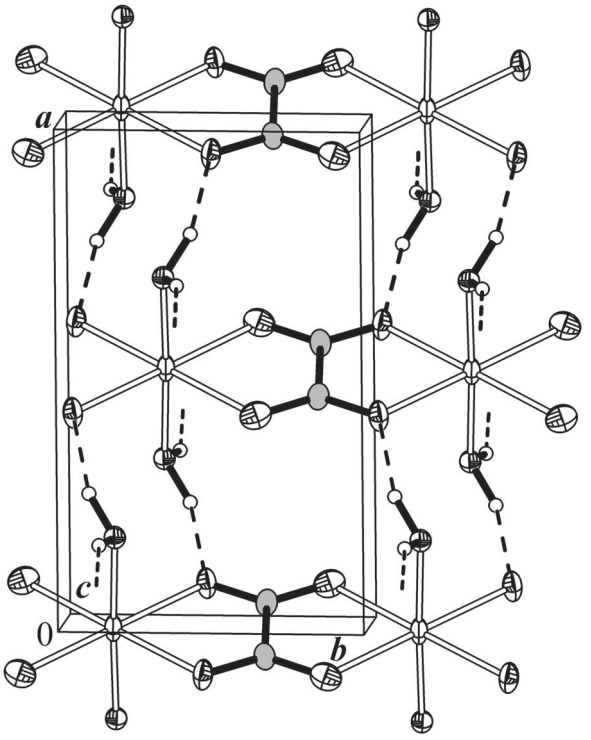

Figure 4. Crystal packing projection down the *c*-axis of synthetic analogue of humboldtine, $Fe(C_2O_4)\cdot 2H_2O$, showing the non-H atom displacement ellipsoids at the 50% probability label. Carbon, oxygen and iron atoms are, respectively, shown by open grey, hatched and crossed ellipsoids. H-bonds are indicated by dashed lines. Atomic parameters were taken from [40].

X-ray diffraction from a synthetic sample [40]. $Fe(C_2O_4)\cdot 2H_2O$ crystallizes in a centred monoclinic lattice (cf. Table 2) and it is isotypic to the manganese(II)-containing mineral lindbergite, $Mn(C_2O_4)\cdot 2H_2O$. A view of synthetic humboldtine crystal is shown in Figure 4. The oxalate molecule is planar and on the same crystallographic two-fold axis as the metal. Iron(II) is at the centre of a slightly distorted octahedral environment (FeO_6 core) in an square coordination with two neighbouring oxalate, symmetry-related to each other by a unit cell translation along the crystal *b*-axis, through their 'bite' carboxylate oxygen atoms, hence giving rise to one-dimensional ... $(C_2O_4)Fe(C_2O_4)$ ... chains in the lattice. The octahedral apical positions are occupied by two water molecules which bridge neighbouring chains through OwH ... O(oxalate) bonds.

The rare mineral minguzzite, of composition $K_3[Fe(C_2O_4)_3]\cdot 3H_2O$, is the natural analogue of one of best characterized and widely investigated oxalate complexes. It was found associated with humboldtine and iron oxides at the ferriferous deposit of Cape Calamita mine (Elba Island, Italy) and was characterized by chemical analysis, goniometric measurements and X-ray powder diffraction [86]. Its crystal structure was investigated by different authors but it was definitively refined in 2005 using a synthetic sample [41].

Two more complex natural oxalates are stepanovite, $NaMg[Fe^{III}(C_2O_4)_3]\cdot 8\text{-}9H_2O$, which occurs in the form of yellowish-green granular aggregates in brown coal deposits in the estuary of the Lena river, polar Yakutia, Russia [43,85,87], and the

related zhemchuzhnikovite, $NaMg[(Al,Fe^{III})(C_2O_4)_3]\cdot 9H_2O$, with Al:Fe = 1.22:0.75. This smoky-green mineral was found in the same geographic region as stepanovite [43,85,88], with which it appears associated. Both minerals were characterized mineralogically and analysed chemically by Knipovich et al. in 1963 [89]. No complete structural analyses for these minerals were performed for decades after its discovery and description.

Synthetic complexes analogous to the minerals stepanovite and zhemchuzhnikovite have never been described in detail as such. Notwithstanding, a complex species of composition $NaMg[Al(C_2O_4)_3]\cdot 9H_2O$ is well known, and has often been used as a host material for different spectroscopic studies, as part of the Al(III) ions can be easily replaced by other trivalent cations (Ti, V, Cr, Mn, Fe, Co) [31,85]. Structural studies on any of these complexes have not been performed yet, although it was shown that $NaMg[Al(C_2O_4)_3]\cdot 9H_2O$ belongs to the trigonal system, and also found that it is isotypic to the analogous Cr(III) compound, an iconic complex in coordination chemistry which has usually been considered as a prototype for this family of oxalate complexes [31,85]. The double sodium and magnesium salt of tris(oxalate) chromate(III) was first obtained by Frossard [90]. From chemical analysis, Frossard reported eight crystallization water molecules and therefore the chemical formula $NaMg[Cr(C_2O_4)_3]\cdot 8H_2O$. Furthermore, using photographic X-ray diffraction data, he determined the crystal system as trigonal and from the observed extinction of reflections, the space group to be either $P\bar{3}1c$ or $P31c$ (differing only in the presence of an inversion centre in the former group) with cell constants (in the hexagonal basis) $a = b = 9.78(4)$ Å, $c = 12.5(2)$ Å, $V = 1033(26)$ Å^3, and $Z = 2$. Frossard ruled out the non-centre space group $P31c$ because the absence of crystal pyroelectricity effects. Mortensen [91] reported that the double salt is in fact a nona rather than an octa hydrate, namely $NaMg[Cr(C_2O_4)_3]\cdot 9H_2O$, and that it crystallizes in either the space group $P\bar{3}1c$ or $P31c$ with $a = b = 16.90(7)$ Å, $c = 12.52(2)$ Å, $V = 3097(31)$ Å^3 and $Z = 6$. As for the Frossard's work, no complete data set of X-ray diffraction intensities was collected to unravel the detailed molecular structure of the salt. Finally, Suh et al. [92] carried out a single crystal X-ray study with a four-circle diffractometer where they report yet another hydrate, $NaMg[Cr(C_2O_4)_3]\cdot 10H_2O$, the same centre-symmetric space group $P\bar{3}1c$ as above and cell constants $a = b = 16.969(3)$ Å and $c = 12.521(3)$ Å. The authors could not locate the water H-atoms in their electron density maps. In a more recent work by Riesen and Rae [93] where the crystal structure of the isotypic $NaMg[Al(C_2O_4)_3]\cdot 9H_2O$ compound is reported, the authors assign the non-centric $P31c$ space group and confirm the nine water molecules, a conclusion that clearly extends to the Cr(III) complex [85,93].

The remaining uncertainties on the $NaMg[Cr^{III}(C_2O_4)_3]\cdot 9H_2O$ solid were finally also removed by X-ray crystallography, confirming the acentric space group $P3c1$ through the above described intrinsic phasing procedure [4], the nine water molecules and uncovering the absolute structure of the salt and its rich H-bonding network as revealed by experimental electron density maps. The crystal structure of isotypic $NaMg[Al(C_2O_4)_3]\cdot 9H_2O$ was also re-determined in the same study [94].

As it was highly probable that stepanovite and zhemchuzhnikovite are isotypic to each other and to the also isotypic $NaMg[Al(C_2O_4)_3]\cdot 9H_2O$ and $NaMg[Cr(C_2O_4)_3]\cdot 9H_2O$ pair, it was attempted to prepare synthetic samples of these two minerals using similar chemical procedures as those employed for the synthesis of the stoichiometrically related Cr(III) and Al(III) complexes. With this synthetic material, the structure of these two rare and interesting minerals could be determined for the first time [44]. A short time later, these

results were confirmed by a similar, independent, study using both natural and synthetic mineral samples [95].

The measurements, performed on an automatic four-circle CCD diffractometer, fully confirmed the above structural expectancies on the synthetic analogues of stepanovite and zhemchuzhnikovite. In fact, an initial molecular model assuming the same *P*3*c*1 space group (again confirmed by intrinsic phasing) and positions of non-H atoms as in the Cr(III)-containing crystal with the identity of the transition metal changed to either iron or a mixture of iron and aluminium lead to smooth convergence of the structural parameters for the synthetic minerals during the least-squares refinement against the corresponding X-ray data set. All 18 water H-atoms in synthetics stepanovite were located among the first 18 most intense peaks of a Fourier difference map phased on the heavier atoms. The H-atoms in synthetic zhemchuzhnikovite were less defined and all of them appeared at approximate locations among the first 25 peaks of the corresponding map. Figure 5 shows an ORTEP drawing of the synthetic analogue of stepanovite. The metal (M) and sodium ions are at crystal general positions, in octahedral environments coordinated to three planar oxalate molecules acting as bidentate ligands through the oxygen atoms of their opposite carboxylic groups in a propeller-like conformation. Because of the crystal three-fold axis, these metal ions are in a honeycomb-like layered arrangement conformed by alternating metal and sodium atoms linked through sharing oxalate ligands (see Figure 5).

There are three different Mg(II) ions positioned at the three special lattice sites of C_3 symmetry in *P*3*c*1 space group and they are at the honeycomb plane. These alkaline-metal ions are in an octahedral environment coordinated to water molecules through their oxygen lone pairs. The three $[Mg(H_2O)_6]^{2+}$ hydrated ions fill the honeycomb holes hence giving rise to an electrically neutral layered structure of about 5.5 Å in width considering van der Waals layer contours. These layers can be conveniently described as $Na[Mg(H_2O)_6][M(C_2O_4)_3]$ and the whole crystal as $Na[Mg(H_2O)_6][M(C_2O_4)_3].3H_2O$. Neighbouring layers are symmetry related to each other through the crystal *c*-glide plane of the *P*3*c*1 space group and therefore they are *c*/2 apart. The layers are weakly bonded to each other mainly through H-bonding bridges involving the remaining three water molecules (see Figure 5 and text below). This explains the easy-cleavage plane parallel to (0001) observed in both synthetic and natural zhemchuzhnikovite mineral [96].

The nine water molecules per chemical formula nicely split into two sets. One of them contains six coordinated-to-magnesium water molecules (O1w to O6w in Figure 5) which in turn can be arranged into three subsets with two molecules each: (O1w, O2w), (O3w, O4w) and (O5w, O6w), respectively, coordinated to the three independent Mg(II) ions at the three C_3 lattice sites giving rise to the above-mentioned $[Mg(H_2O)_6]^{2+}$ hydrated ions. The other set contains the remaining three molecules which act as crystallization waters (O7w to O9w). They are sandwiched between neighbouring $Na[Mg(H_2O)_6][M(C_2O_4)_3]$ crystal layers bridging them through relatively strong H-bonds. In fact, all three water molecules act as H-donors in O(ox) ... H–Ow–H ... O(ox) bridges with oxalate oxygen atoms.

2.6.4. Lanthanide-containing oxalates

There are a series of very interesting oxalate minerals, described some years ago, which are unique in two respects: they are the first natural lanthanide oxalates and the first natural double salts of two acids, one organic and the other inorganic. They appear

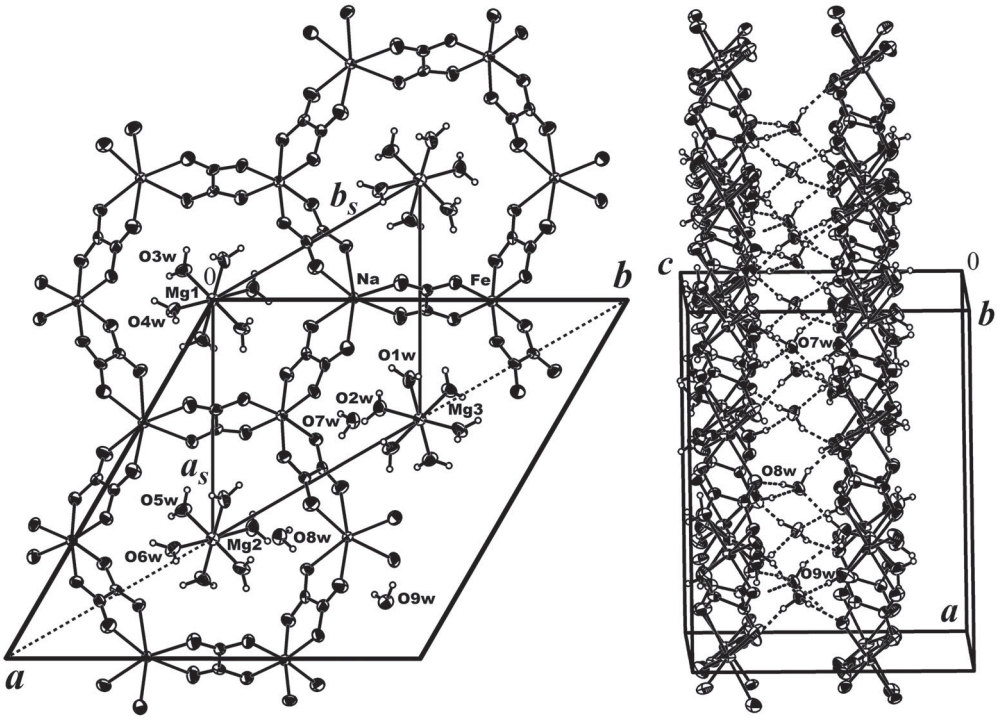

Figure 5. *Left:* view of synthetic analogue of stepanovite, $Na[Mg(H_2O)_6][Fe(C_2O_4)_3].3H_2O$, down the crystal trigonal axis, showing the displacement ellipsoids at the 50% probability level. The crystallographic c-glide plane relating neighbouring $Na[Mg(H_2O)_6][Fe(C_2O_4)_3]$ crystal layers along the *c*-axis is shown by dotted lines. The trigonal (a_S, b_S) sub-cell early reported for the mineral is shown by thin lines embedded in the correct (*a*, *b*) cell. *Right*: view perpendicular to the trigonal axis. The crystal layered arrangement is seen edge-on. The H-bonding structure linking neighbouring layers through bridging water molecules is indicated by dashed lines. Drawing reproduced from Figure 1 of [44] with permission kindly granted by Springer.

in cavities as embedded or free standing crystals mixed with epsomite and the so-called hair salts. These minerals are coskrenite-(Ce), $(Ce,Nd,La)_2(SO_4)_2(C_2O_4)\cdot 8H_2O$ [31,45], levinsonite-(Y), $(Y,Nd,Ce)Al(SO_4)_2(C_2O_4)\cdot 12H_2O$ [31,46] and zugshunstite-(Ce), $(Ce,Nd,La)Al(SO_4)_2(C_2O_4)\cdot 12H_2O$ [31,46]. The last two have a special crystal chemical significance in having the same complex formula type but different crystal structures, generated by the presence of the lower or higher weight lanthanide cations.

Synthetic counterparts of these interesting mineral species have so far not been reported, a fact which is probably related to the experimental difficulties arising from the high insolubility of the lanthanide oxalates.

Most recently, a new lanthanide-containing oxalate, named deveroite-(Ce) and formulated as $Ce_2(C_2O_4)_3\cdot 10H_2O$ was found in Mount Cervandone (Devero Valley, Western-Central Alps, Italy). Besides cerium, it contains traces of other lanthanides, as well as thorium, uranium, lead and calcium [47]. The mineral crystallizes in the monoclinic space group $P2_1/c$ with $Z = 2$ and it is, therefore, isostructural with some other known synthetic lanthanide oxalates of the same stoichiometry, namely $Ln_2(C_2O_4)_3\cdot 10H_2O$ (Ln = La, Pr, Nd), prepared and characterized a long time ago [48].

2.6.5. Kyanoxalite

A mineral species named kyanoxalite, with the idealized formula $Na_7[(Al_{5-6}Si_{6-7}O_{24})(C_2O_4)_{0.5-1}]\cdot 5H_2O$, was found in hydrothermally altered hyper-alkaline rocks and pegmatites of the Lovozero massif, Kola Peninsula, Russia [49]. This mineral represents the first natural aluminosilicate containing an organic acid anion.

The cancrinite-group of minerals is abundant in igneous rocks of alkaline complexes, both intrusive and volcanic and is especially characteristic of post-magmatic assemblages related to these rocks. The cancrinite-group members, displaying highly variable chemical composition and crystal structure, are important geochemical and petrological indicators [49,97]. The group involves hexagonal and trigonal feldspathoids, in the zeolitic cavities of which additional anions (CO_3^{2-}, SO_4^{2-}, OH^-, Cl^- and S^{2-}) and in most cases water molecules are located along with cations, largely sodium, potassium and calcium. The frameworks consist of six-member rings of AlO_4 and SiO_4 tetrahedral units arranged on the *xy* plane [97]. The distinctive feature of kyanoxalite is the presence of $C_2O_4^{2-}$ groups as major extra framework anions [49].

3. Conclusions

From the above review, we can draw the following major conclusions:

(1) On the one hand, detailed crystal structure determination by X-ray diffraction of several synthetic analogues of organic minerals was carried out before the discovery of their natural counterparts. This is the case of the two known natural formates formicaite β-$Ca(HCOO)_2$ and dashkovaite, $Mg(HCOO)_2\cdot 2H_2O$; the natural acetates, namely hoganite, $Cu(CH_3COO)_2\cdot H_2O$, and paceite, $CaCu(CH_3COO)_4\cdot 6H_2O$; the only known natural alkaline oxalate natroxalate, $Na_2C_2O_4$; the calcium oxalate mineral caoxite, $Ca(C_2O_4)\cdot 3H_2O$; and the natural Mn(II) oxalate lindbergite, $MnC_2O_4\cdot 2H_2O$.

(2) On the other hand, complete crystal structure determination of early discovered organic minerals was made possible through the advent of combined synthetic chemistry and advanced X-ray diffraction methods to remove the uncertainties associated with natural samples and the limitations of old data collection instruments and structure determination and refinement procedures. This is the case of the only known natural citrate earlandite, $[Ca_3(C_6H_5O_7)_2(H_2O)_2]\cdot 2H_2O$; the methanesulfonate ernstburkeite, $Mg(CH_3SO_3)_2\cdot 12H_2O$; the oxalate oxammite, $(NH_4)_2C_2O_4\cdot H_2O$; the Mn(II) oxalate falottaite, $MnC_2O_4\cdot 3H_2O$; the Fe(II) oxalate, humboldtine, α-$Fe^{II}(C_2O_4)\cdot 2H_2O$; the Fe(III) oxalates minguzzite, $K_3[Fe(C_2O_4)]\cdot 3H_2O$; and the isotypic to each other stepanovite, $NaMg[Fe(C_2O_4)_3]\cdot 9H_2O$, and zhemchuzhnikovite, $NaMg[(Al,Fe)(C_2O_4)_3]\cdot 9H_2O$.

(3) The crystal structures of a few organic minerals were solved as part of its characterization and published along with their discovery. This is the case of mellite, $Al_2[(C_6(COO)_6]\cdot 16H_2O$, and novgorodovaite, $Ca_2(C_2O_4)Cl_2\cdot 2H_2O$. It turned out that the synthetic novgorodovaite and its heptahydrate analogue, $Ca_2(C_2O_4)Cl_2\cdot 7H_2O$, were prepared and characterized, including powder X-ray diffraction *d*-spacings, 55 years before the discovery of the mineral. Recent crystal

structure determination of both synthetic calcium oxalate hydrates proved the monohydrate to be identical to the natural counterpart. Also, and after 70 years since the report of its preparation, it was disclosed the detailed crystal structure of the heptahydrate analogue of novgorodovaite, namely $Ca_2(C_2O_4)Cl_2{\cdot}7H_2O$, whose crystals grow as triclinic ($P\bar{1}$) twins. This probably hampered early attempts of crystal structure determination and refinement due to the difficulties in collecting diffraction data from multiple single crystal domains employing photographic or scintillation-counter methods, and also to the lack of untwining procedures during crystal structure refinement. Because the heptahydrate crystal arises under the same preparative conditions that also produces the novgorodovaite analogue, it is tempting to speculate that $Ca_2(C_2O_4)Cl_2{\cdot}7H_2O$ could be the synthetic analogue of a mineral yet to be discovered.

(4) After over 60 and 50 years, respectively, since their discovery, combined chemical synthesis and modern X-ray diffraction methods afforded to disclose the structural beauty and complexity of stepanovite, $NaMg[Fe^{III}(C_2O_4)_3]{\cdot}9H_2O$, and zhemchuzhnikovite, $NaMg[(Al,Fe^{III})(C_2O_4)_3]{\cdot}9H_2O$, minerals and their isotypic relationship with each other and with the synthetic $Na[Mg(H_2O)_6][M(C_2O_4)_3]{\cdot}3H_2O$ (M: Cr, Al) complexes.

(5) We conclude that synthetic chemistry of mineral analogues, followed by advanced single crystal X-ray diffraction methods provides a powerful approach to uncover the full crystal and molecular structure of natural minerals, thus filling the gaps that still remain in the characterization of these materials, the mutual relation among them and with other synthetic materials, and also providing structural information on related natural analogues hitherto undiscovered.

Acknowledgements

Oscar E. Piro is a Research Fellow of CONICET.

Disclosure statement

No potential conflict of interest was reported by the authors.

Funding

We thank CONICET – Consejo Nacional de Investigaciones Científicas y Técnicas [grant number PIP 11220130100651CO] and UNLP – Universidad Nacional de La Plata [grant numbers 11/X709 and 11/X673] of Argentina for financial support.

Notes on contributors

Oscar E. Piro received his Doctorate in Physics (PhD) from the National University of La Plata (UNLP), Argentina, in 1977, in the field of Solid State Physics. He made post-doctoral research at the Department of Biophysics and Theoretical Biology of the University of Chicago, working on X-ray crystallography of biological macromolecules (1978–1980). He is one of the pioneers in the information theoretical approach (maximum entropy) to the solution of the 'phase problem'. Upon his return to Argentina he became a Research Fellow of CONICET and currently he is Full Professor of UNLP. His research interest

is grounded in Solid State Physics, particularly in Structural Crystallography by X-ray diffraction methods and also in the optical and spectroscopic (mainly infrared and Raman) properties of crystals. Currently, he works on the structure-physicochemical properties relationship of inorganic, organic, metal-organic (including minerals), bioorganic and bioinorganic, pharmaceutical (both natural and synthetic), supra-molecular and liquid crystal materials.

Enrique J. Baran received his Doctorate in Chemistry (PhD) from the National University of La Plata (UNLP), Argentina, in 1967, in the field of Inorganic Chemistry. He made post-doctoral research at the Institute of Inorganic Chemistry, University of Göttingen (1968–1970) and at the Faculty of Chemistry, University of Dortmund (1974), in both opportunities under the supervision of Prof. Achim Müller. Full Professor of Inorganic Chemistry (1981–2005) and Emeritus Professor of the UNLP (2008). Research Fellow from CONICET (1970–2012). Visitant Professor in Universities of Colombia, Germany, Spain and Uruguay. Director of the Center of Inorganic Chemistry-CEQUINOR (2001–2006). Member of the National Academy of Exact, Physical and Natural Sciences (1996-cont.) and of TWAS (1997-cont.). National Representative at IUPAC (1984–1992). Author of the first text book on Inorganic Biochemistry, in Spanish language (1995) and of more than 700 scientific publications. His main research interests include coordination chemistry, solid state chemistry, biomineralization, vibrational spectroscopy, bioinorganic chemistry and medicinal inorganic chemistry.

References

[1] Bragg WL. The structure of some crystals as indicated by their diffraction of X-rays. Proc R Soc. 1913;A89:248–277.
[2] Sheldrick GM, Gould RO. Structure solution by iterative peaklist optimization and tangent expansion in space group *P*1. Acta Cryst. 1995;B51:423–431.
[3] Burla MC, Carrozzini B, Cascarano GL, et al. Solving crystal structures in P1: an automated procedure for finding an allowed origin in the correct space group. J Appl Cryst. 2000;33:307–311.
[4] Palatinus L, van der Lee A. Symmetry determination following structure solution in *P*1. J Appl Cryst. 2008;41:975–984.
[5] Sheldrick GM. SHELXT – integrated space-group and crystal structure determination. Acta Cryst. 2015;A71:3–8.
[6] Strunz H, Nickel EH. Strunz mineralogical tables. 9th ed. Stuttgart: Schweizerbart'sche Verlagsbuchhandlung; 2001.
[7] Chukanov NV, Malinko SV, Lisitsyn AE, et al. Formicaite $Ca(HCOO)_2$, a new mineral. Zapiski Vseross Mineral Obshch. 1999;128:43–47. (in Russian).
[8] Jambor JL, Pertsev NN, Roberts AC. New mineral names. Amer Mineral. 2000;85:1321–1325.
[9] Matsui M, Watanabé T, Kamijo N, et al. The structures of calcium formate β-$Ca(HCOO)_2$ and δ-$Ca(HCOO)_2$ and the tetragonal mixed crystals $Ca(HCOO)_2$ – $Sr(HCOO)_2$. Acta Cryst. 1980;36B:1081–1086.
[10] Chukanov NV, Belakovsky DI, Malinko SV, et al. Dashkovaite $Mg(HCOO)_2{\cdot}2H_2O$ – A new formate mineral. Zapiski Vseross Mineral Obshch. 2000;129:49–53. (in Russian).
[11] Jambor JL, Roberts AC. New mineral names. Amer Mineral. 2001;86:1534–1537.
[12] Mandarino JA. New minerals. Canad Mineral. 2001;39:1473–1502.
[13] De With G, Harkema S, van Hummel GJ. Magnesium formate dihydrate: a crystal structure redetermination at 130 and 293 K. Acta Cryst. 1976;32B:1980–1983.
[14] Hibbs DE, Kolitsch U, Leverett P, et al. Hoganite and paceite: two new acetate minerals from the Potosi mine Broken Hill, Australia. Mineral Mag. 2002;66:459–464.
[15] Brown GM, Chidambaram R. Dinuclear copper(II) acetate monohydrate: a determination of the structure by neutron-diffraction analysis. Acta Cryst. 1973;B29:2393–2403.
[16] Klop EA, Duisenberg AJM, Spek AL. Reinvestigation of the structure of calcium copper acetate hexahydrate, $CaCu(CH_3COO)_4.6H_2O$. Acta Cryst. 1983;C39:1342–1344.

[17] Giuseppetti G, Tadini C, Ungaretti L. La struttura cristallina della calclacite. Per Mineral. 1970;39:145–158.
[18] Herdtweck E, Kornprobst T, Sieber R, et al. Crystal structure, synthesis, and properties of *tri*-calcium *di*-citrate *tetra*-hydrate $[Ca_3(C_6H_5O_7)_2(H_2O)_2]\cdot 2H_2O$. Z Anorg Allg Chem. 2011;637:655–659.
[19] Giacovazzo C, Menchetti S, Scordari F. The crystal structure of mellite. Amer Mineral. 1973;B29:26–31.
[20] Plater MJ, Harrison WTA. A geomimetic synthesis of mellite: a mineral containing a benzene ring. J Chem Res. 2015;39:279–281.
[21] Genceli FE, Lutz M, Sakurai T, et al. Crystallization and characterization of magnesium methanesulfonate hydrate $Mg(CH_3SO_3)_2.12H_2O$. Cryst Growth Des. 2010;10:4327–4333.
[22] Khomyakov AP. Natroxalate, $Na_2C_2O_4$, a new mineral. Zapiski Vseross Mineral Obshch. 1996;125:126–132. (in Russian).
[23] Jambor JL, Pertsev NN, Roberts AC. New mineral names. Amer Mineral. 1997;82:430–433.
[24] Reed DA, Olmstead MM. Sodium oxalate structure refinement. Acta Cryst. 1981;B37: 938–939.
[25] Tazzoli V, Domeneghetti C. The crystal structures of whewellite and wheddellite: re-examination and comparison. Amer Mineral. 1980;65:327–334.
[26] Deganello S, Piro OE. The crystal structure of calcium oxalate monohydrate (whewellite). Neues Jahrb Mineral Monatsh. 1981;2:81–88.
[27] Basso R, Lucchetti G, Zefiro L, et al. Caoxite, $Ca(H_2O)_3(C_2O_4)$, a new mineral from Cerchiara mine, northern Apennines, Italy. Neues Jahrbuch für Mineralogie Abhandlungen. 1997;2:84–96.
[28] Conti C, Casati M, Colombo C, et al. Synthesis of calcium oxalate trihydrate: new data by vibrational spectroscopy and synchrotron X-ray diffraction. Spectrochim Acta. 2015;150A: 721–730.
[29] Rastsvetaeva RK, Chukanov NV, Nekrasov Y. Crystal structure of novgorodovaite $Ca_2(C_2O_4)Cl_2\cdot 2H_2O$. Doklady Chem. 2001;381:329–331.
[30] Piro OE, Echeverría GA, González-Baró AC, Baran EJ. Crystal structure and spectroscopic behaviour of synthetic novgorodovaite $Ca_2(C_2O_4)Cl_2\cdot 2H_2O$ and its twinned triclinic heptahydrate analogue. Phys Chem Min. 2018;45:185–195.
[31] Baran EJ. Review: natural oxalates and their analogous synthetic complexes. J Coord Chem. 2014;67:3734–3768.
[32] Taylor JC, Sabine TM. Isotope and bonding effects in ammonium oxalate monohydrate determined by the combined use of neutron and X-ray diffraction analysis. Acta Cryst. 1972;B28:3340–3351.
[33] Atencio D, Coutinho JMV, Graesser S, et al. Lindbergite, a new Mn oxalate dihydrate from Boca Rica mine, Galiléia, Minas Gerais, Brazil, and other occurrences. Amer Mineral. 2004;89:1087–1091.
[34] Soleimannejad J, Aghabozorg H, Hooshmand S, et al. The monoclinic polymorph of *catena*-poly [[diaquamanganese(II)]-μ-oxalato-κ^4 O^1,O^2: $O^{1'}$,$O^{2'}$]. Acta Cryst. 2007;E63: m2389–m2390.
[35] Fu X, Wang C, Li M. *catena*-Poly[[[diaquamanganese(II)]-μ-oxalato] monohydrate]. Acta Crystallogr. 2005;E61:m1348–m1349.
[36] Christensen AN, Lebech B, Andersen NH, et al. The crystal structure of paramagnetic copper(II) oxalate (CuC_2O_4): formation and thermal decomposition of randomly stacked anisotropic nano-sized crystallites. Dalton Transact. 2014;43:16754–16768.
[37] Rouse RC, Peacor DR, Dunn PJ, et al. Wheatlyite, $Na_2Cu(C_2O_4)_2\cdot 2H_2O$, a natural sodium copper salt of oxalic acid. Amer Mineral. 1986;71:1240–1242.
[38] Gleizes MF, Galy J. Crystal structure and magnetism of sodium bis(oxalato)cuprate(II) dehydrate, $Na_2Cu(C_2O_4)_2\cdot 2H_2O$. A deductive proposal for the structure of copper oxalate $CuC_2O_4\cdot xH_2O$ ($0 \leq x \leq 1$). Inorg Chem. 1980;19:2074–2078.
[39] Chukanov NV, Aksenov SM, Rastsvetaeva RK, et al. Antipinite, $NaK_3Cu_2(C_2O_4)_4$, a new mineral species from a guano deposit at Pabellón de Pica, Chile. Mineral Mag. 2015;79:1111–1121.

[40] Echigo T, Kimata M. Single crystal X-ray diffraction and spectroscopic studies on humboldtine and lindbergite: weak Jahn-Teller effect of Fe^{2+} ion. Phys Chem Min. 2008;35:467–475.
[41] Junk P C. Supramolecular interactions in the X-ray crystal structure of potassium tris(oxalato)ferrate(III) trihydrate. J Coord Chem. 2005;58:355–361.
[42] Anthony JW, Bideaux RA, Bladh KW, Nichols MC. Handbook of mineralogy, online version. Chantilly, VA: Mineralogical Society of America, c 2004–2011. http://www.handbookofmineralogy.org/
[43] Fleischer M. New mineral names: zhemchuzhnikovite, stepanovite. Amer Mineral. 1964;49:442–443.
[44] Piro OE, Echeverría GA, González-Baró AC, et al. Crystal and molecular structure and spectroscopic behaviour of isotypic synthetic analogs of the oxalate minerals stepanovite and zhemchuzhnikovite. Phys Chem Min. 2016;43:287–300.
[45] Peacor DR, Rouse RC, Essene EJ. Coskrenite-(Ce), $(Ce,Nd,La)_2(C_2O_4)\cdot 8H_2O$, a new rare-earth oxalate mineral from Alum Cave Bluff, Tennessee: characterisation and crystal structure. Canad Mineral. 1999;37:1453–1462.
[46] Rouse RC, Peacor DR, Essene EJ, et al. The new minerals levinsonite-(Y) $[(Y,Nd,Ce)Al(SO_4)_2(C_2O_4)\cdot 12H_2O]$ and zugshunstite-(Ce)$[(Ce,Nd,La)Al(SO_4)_2(C_2O_4)\cdot 12H_2O]$: coexisting oxalates with different structures and differentiation of LREE and HREE. Geochim Cosmochim Acta. 2001;65:1101–1115.
[47] Guastoni A, Nestola F, Gentile P, et al. Deveroite-(Ce): A new RRE-oxalate from Mount Cervandone, Devero Valley, Western-Central Alps, Italy. Mineral Mag. 2013;77:3019–3026.
[48] Ollendorff W, Weigel F. The crystal structure of some lanthanide oxalate decahydrates, $Ln_2(C_2O_4)_3\cdot 10H_2O$, with Ln = La, Ce, Pr, Nd. Inorg Nucl Chem Lett. 1969;5:263–269.
[49] Chukanov NV, Pekov IV, Olysych LV, et al. Kyanoxalite, a new cancrinite-group mineral species with extra framework oxalate anion from the Lovozero alkaline pluton, Kola Peninsula. Geol Ore Dep. 2010;52:778–790.
[50] Comel C, Mentzen BF. Comparative study of the polymorphic species of strontium and calcium formates. I. Differential thermal analysis (DTA). J Solid State Chem. 1974;9:210–213.
[51] Mentzen BF, Comel C. Comparative study of the polymorphic species of strontium and calcium formates. II. X-ray diffraction. J Solid State Chem. 1974;9:214–223.
[52] Cotton FA, Wilkinson G, Murillo CA, et al. Advanced inorganic chemistry. 6th ed. New York: Wiley; 1999.
[53] van Niekerk JN, Schoening FRL. A new type of copper complex as found in the crystal structure of cupric acetate, $Cu_2(CH_3COO)_4.2H_2O$. Acta Cryst. 1953;6:227–232.
[54] van Tassel R. Une efflorescence d'acetochlorure de calcium sur des roches calcaires dans des collections. Bull Musée Royal d'Histoire Naturelle de Belgique. 1945;21:1–11.
[55] van Tassel R. On the crystallography of calclacite, $Ca(CH_3COO)Cl.5H_2O$. Acta Cryst. 1958;11:745–746.
[56] Bannister MA. Report on some crystalline components of the Weddell Sea deposits. Discovery Rep. 1936;13:60–69.
[57] Pogainis EM, Shaw EH, Jr. The unit-cell dimensions of tricalcium citrate tetrahydrate. Proc S Dakota Acad Sci. 1957;36:56–59.
[58] Barth TFW, Ksanda CJ. Crystallographic data on mellite. Amer Mineral. 1933;18:8–13.
[59] Jehlička J, Edwards HGM. Raman spectroscopy as a tool for the non-destructive identification of organic minerals in the geological record. Organ Geochem. 2008;39:371–386.
[60] Genceli FE, Sakurai T, Hondoh T. Ernstburkeite, $Mg(CH_3SO_3)_2.12H_2O$, a new mineral from Antarctica. Eur J Mineral. 2013;25:79–84.
[61] Echigo T, Kimata M. Crystal chemistry and genesis of organic minerals: a review of oxalate and polycyclic aromatic hydrocarbon minerals. Can Mineral. 2010;48:1329–1358.
[62] Baran EJ, Monje PV. Oxalate biominerals. In: Sigel A, Sigel H, Sigel RKO, editors. Metal ions in life sciences, vol. 4. Chichester: Wiley; 2008. p. 219–254.
[63] Beagley B, Small RWH. The structure of lithium oxalate. Acta Cryst. 1964;17:783–788.
[64] Jeffrey GA, Parry GS. The crystal structure of sodium oxalate. J Am Chem Soc. 1954;76:5283–5286.

[65] Dinnebier RE, Vensky S, Panthöfer JM. Crystal and molecular structures of alkali oxalates: first proof of a staggered oxalate anion in the solid state. Inorg Chem. 2003;42:1499–1507.
[66] Khan SR, editor. Calcium oxalate in biological systems. Boca Raton, FL: CRC-Press; 1995.
[67] Monje PV, Baran EJ. Plant biomineralization. In: Hemantaranjan A, editor. Advances in plant physiology, vol. 7. Johdpur: Science Publishers; 2004. p. 395–410.
[68] Franceschi VR, Nakata PA. Calcium oxalate in plants: formation and function. Ann Rev Plant Biol. 2005;56:41–71.
[69] He H, Veneklaas EJ, Kuo J, et al. Physiological and ecological significance of biomineralization in plants. Trends Plant Sci. 2014;19:166–174.
[70] Streit J, Tran-Ho LC, Königsberger E. Solubility of the three calcium oxalate hydrates in sodium chloride solutions and urine-like liquors. Monatsh Chem. 1998;129:1225–1236.
[71] Deganello S. The basic and derivative structures of calcium oxalate monohydrate. Z Kristallogr. 1980;152:247–252.
[72] Mills SJ, Christy AG. The great barrier reef expedition 1928-29: the crystal structure and occurrence of weddellite, ideally $CaC_2O_4{\cdot}2.5H_2O$, from the Low Isles, Queensland. Mineral Mag. 2016;80:399–406.
[73] Hammarsten G. On calcium oxalate and its solubility in the presence of inorganic salts with special reference to the occurrence of oxaluria. C R Lab Carlsberg. 1929;17:1–85.
[74] Deganello S, Kampf AR, Moore PB. The crystal structure of calcium oxalate trihydrate: $Ca(H_2O)_3C_2O_4$. Amer Mineral. 1981;66:859–865.
[75] Lafuente B, Downs RT, Yang H, et al. The power of databases: the RRUFF project, Chapter 1. In: Armbruster T, Danisi RM, editor. Highlights in mineralogical crystallography. Berlin: De Gruyter; 2015. p. 1–29.
[76] Jones FT, White LM. The composition, optical and crystallographic properties of two calcium oxalate-chloride double salts. J Am Chem Soc. 1946;68:1339–1342.
[77] Farrugia LJ. ORTEP-3 for windows – a version of ORTEP-III with a graphical user interface (GUI). J Appl Cryst. 1997;30:565–566.
[78] Winchell H, Benoit RJ. Taylorite, mascagnite, aphthitalite, lecontite and oxamite from guano. Amer Mineral. 1951;36:590–602.
[79] Huizing A, van Hal HAM, Kewstroo W, et al. Hydrates of manganese(II) oxalate. Mat Res Bull. 1977;12:605–611.
[80] Williams PA, Hatert F, Pasero M, et al. New mineral names. CNMNC Newslett. 2013;17:3000.
[81] Graeser S, Gabriel W. Falottaite ($MnC_2O_4{\cdot}3H2O$) - ein neues Oxalat-Mineral aus den schweizerischen Alpen. Schweizer Strähler. 2016;50:20–27.
[82] Wu W-Y, Song Y, Li Y-Z, et al. One-dimensional structure and long-range antiferromagnetic behaviour of manganese(II) oxalate trihydrate: $\{[Mn(\mu\text{-ox})(H_2O)_2]{\cdot}H_2O\}_n$. Inorg Chem Comm. 2005;8:732–736.
[83] Clarke RM, Williams IR. Moolooite, a naturally occurring hydrated copper oxalate from Western Australia. Mineral Mag. 1986;50:295–298.
[84] Michalowicz A, Girerd JJ, Goulon J. EXAFS [extended X-ray absorption fine structure] determination of the structure of copper oxalate. Relation between structure and magnetic properties. Inorg Chem. 1979;18:3004–3010.
[85] Baran EJ. Natural iron oxalates and their analogous synthetic counterparts: a review. Chem Erde – Geochem. 2016;76:449–460.
[86] Garavelli C L. Un nuovo minerali tra i prodotti secondari del giacimento di Cape Calamita (Isola d'Elba). Atti Accad Naz Linzei. 1955;18:392–402.
[87] Fleischer M. New mineral names: Stepanovite. Amer Mineral. 1995;40:551.
[88] Fleischer M. New mineral names: Zhemchuzhnikovite. Amer Mineral. 1962;47:1482–1483.
[89] Knipovich YN, Komkov AI, Nefedov EI. On stepanovite and a new mineral, zhemchuzhnikovite. Trudy Vsegel, Mineralogicheskiy Sbornik. 1963;96:131–135. (in Russian).
[90] Frossard L. Etude du trioxalatochrominate de sodium et de magnésium. Schweiz Mineral Petrog Mitt. 1956;36:1–25.
[91] Mortensen OS. Vibronic spectra of transition metal complexes I. Polarized emission and absorption spectra of $NaMg[Cr(C_2O_4)_3]{\cdot}9H_2O$. J Chem Phys. 1967;47:4215–4222.

[92] Suh J-S, Shin J-Y, Yoon C, et al. The crystal and molecular structure of sodium magnesium tris(oxalate)chromate(III) decahydrate, $NaMg[Cr(ox)_3]\cdot 10H_2O$. Bull Korean Chem Soc. 1994;15:245–249.
[93] Riesen H, Rae D. Revisiting the crystal structure and thermal properties of $NaMgAl(oxalate)_3\cdot 9H_2O$/Cr(III): an extraordinary spectral hole-burning material. Dalton Trans. 2008;26:4717–4722.
[94] Piro OE, Echeverría GA, González-Baró AC, et al. Crystallographic new light on an old complex: $NaMg[Cr(oxalato)_3]\cdot 9H_2O$ and structure redetermination of the isomorphous aluminum(III) compound. J Coord Chem. 2015;68:3776–3787.
[95] Huskić I, Pekov IV, Krivovichev SV, et al. Minerals with metal-organic framework structures. Sci Adv. 2016;2:e1600621.
[96] Fleischer M. New mineral names. Am Mineral. 1964;49:439–448.
[97] Pekov IV, Olysych LV, Chukanov NV, et al. Crystal chemistry of cancrinite-group minerals with an AB-type framework: A review and new data. I. Chemical and structural variations. Can Mineral. 2011;49:1129–1150.

Subject index of terms